Fault-Tolerant Event-Triggered $\mathcal{H}_\infty$ Load Frequency Control for Multiarea Power Systems With Communication Delay

Hao Shen, *Member, IEEE*, Yude Xia, Jing Wang, and Ju H. Park, *Senior Member, IEEE*

***Abstract*—This article addresses the $\mathcal{H}_\infty$ load frequency control problem for multiarea power systems. In order to reduce the heavy burden of the communication channel and relieve the impact caused by the actuator failures, an event-triggered mechanism and a fault-tolerant strategy are adopted, simultaneously. The main purpose is to design a controller so that the multiarea power systems are asymptotically stable in the case of actuator failures and communication delays. On the basis of the Lyapunov stability theory, some sufficient criteria for ensuring the stability of the synthesized system with an expected $\mathcal{H}_\infty$ performance are obtained. Finally, the effectiveness and feasibility of the proposed method are demonstrated via an illustrative example.**

***Index Terms*—Event-triggered mechanism, fault-tolerant $\mathcal{H}_\infty$ control, load frequency control, power systems.**

I. Introduction

ROUGHLY speaking, the load frequency control (LFC) scheme may keep the power and frequency of the adjacent interval reaching the required nominal value to ensure the quality of the energy supply for power systems (PSs). As a consequence, it is an effective way to deal with the frequency fluctuations caused by time-varying loads and slow changes in the input power of the prime mover. Naturally, the past few decades have witnessed an important progress on such a topic, see, for instance, [1]–[6] and the references therein.

The traditional LFC scheme generally applies dedicated communication channels, which is not applicable to the large-scale PSs, and apparently, is inadequate for their efficiency. In this regard, the highly open communication infrastructure is pressingly demanded by the market [7], [8]. Different from the traditional LFC scheme, the modern one with open communication infrastructure may realize the large-scale information exchange. However, it is noted that the open communication infrastructure also has some inadequacies such as the discontinuous transmission of data, disorder, and data packet loss [9]. These inadequacies may be caused by the network congestion and collision, which can affect the real-time execution of information exchange and lead to the occurrence of time delays [10]–[13]. In view of this, many scholars devote themselves to the LFC problem for delayed PSs. To name just a few, the authors in [14] proposed an improved way to analyze the stability of delayed PSs under the LFC scheme. The LFC problem for PSs with communication delay via an event-triggered communication scheme (ETCS) was discussed in [15].

Additionally, the bandwidth of an open communication network among the multiple subunits is limited. Therefore, a question with practical significance is raised, that is, *how to save bandwidth while guaranteeing the expected performance of PSs?* To save this problem, the ETCS is adopted for the LFC for PSs [16]–[19]. Compared with the time-triggered scheme, which transmits all sampled-data (SD) directly, the ETCS can reduce the data transmission by setting a trigger condition, and accordingly economizes the bandwidth resources [20]–[26]. For example, the authors in [27] researched the LFC problem for PSs under ETCS, where the hybrid attack strategy was involved. As stated in [28], the ETCS on the basis of the observer design for the LFC problem in multiarea PSs with the $\mathcal{L}_\infty$ performance was concerned.

It is noted that the above-mentioned results ignore the effects of actuator faults. However, actuator faults are inevitable due to the influence of the external environment and the aging of the equipment, and actuator faults may lead to system instability

Manuscript received 27 July 2021; revised 5 November 2021 and 15 December 2021; accepted 29 January 2022. Date of publication 1 March 2022; date of current version 9 December 2022. This work was supported in part by the National Natural Science Foundation of China under Grant 62173001, Grant 61703004, and Grant 61873002, in part by the Major Natural Science Foundation of Higher Education Institutions of Anhui Province under Grant KJ2020ZD28, in part by the Natural Science Foundation for Excellent Young Scholars of Anhui Province under Grant 2108085Y21, in part by the Major Technologies Research and Development Special Program of Anhui Province under Grant 202003a05020001, in part by the Fundamental Research Funds for the Central Universities. The work of J. H. Park was supported by the National Research Foundation of Korea (NRF) Grant Funded by the Korea Government, Ministry of Science and ICT under Grant 2019R1A5A8080290. *(Corresponding authors: Ju H. Park; Jing Wang.)*

Hao Shen is with the School of Electrical and Information Engineering, Anhui University of Technology, Ma'anshan 243032, China, and also with the Key Laboratory of Advanced Control and Optimization for Chemical Processes, Ministry of Education, East China University of Science and Technology, Shanghai 200237, China (e-mail: haoshen10@gmail.com).

Yude Xia is with the School of Electrical and Information Engineering, Anhui University of Technology, Ma'anshan 243032, China (e-mail: xiayude829@163.com).

Jing Wang is with the School of Electrical and Information Engineering, Anhui University of Technology, Ma'anshan 243032, China, and also with the School of Automation and Electrical Engineering, Linyi University, Linyi 276005, China (e-mail: jingwang08@126.com).

Ju H. Park is with the Department of Electrical Engineering, Yeungnam University, Kyongsan 38541, South Korea (e-mail: jessie@ynu.ac.kr).

Digital Object Identifier 10.1109/JSYST.2022.3149566

TABLE I
NOTATIONS EMPLOYED FOR iTH AREA LFC MODEL

M_i	inertia constant
R_i	droop property
$\triangle f_i(t)$	frequent deviation
T_{chi}	turbine time constant
D_i	generator damping factor
$\triangle P_{tie-i}(t)$	power flow with net tie-line
$\triangle P_{vi}(t)$	positional deviation of valve
$\triangle P_{di}(t)$	disturbance deviation for load
T_{gi}	synchronization factor in tie-line
$\triangle P_{mi}(t)$	mechanical output deviation for generator

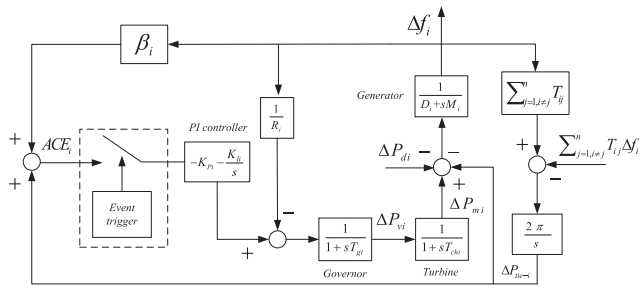

Fig. 1. Diagram of the ith control area of LFC for multiarea PSs under ETCS.

[29]–[32]. As a sequence, many experts and scholars focus on the fault-tolerant control strategy (FTCS). At present, the FTCS mainly includes active fault-tolerant control and the passive one. Thereinto, there are three main types of active fault-tolerant control based on the reconfiguration rules of fault-tolerant controllers: control-law rescheduling, control-law reconfiguration design, and model-tracking reconfiguration control. However, this control strategy needs to design more control algorithms. Thus, a passive FTCS is adopted in this article, which allows the occurrence of malfunctions within certain limits in systems, and makes systems more reliable. For example, as considered in [33], the FTCS was proposed to deal with the static output feedback control (SOFC) problem. To best of authors' knowledge, there are few research on FTCS for PSs. Thus, a meaningful question arises: *how to combine the $FTCS$ with the ETCS to address the $\mathcal{H}_\infty LFC$ problem for PSs?* This motivates this article.

This article aims to associate FTCS and ETCS into multiarea PSs with an $\mathcal{H}_\infty$ performance. The contributions are stated in the following.

a) A PI-type controller is designed for the PSs with a three-area delayed LFC scheme, and the corresponding stability criterion is derived by using Lyapunov stability theory and optimization inequality techniques. Moreover, the relationships among the event-triggered parameter α, the upper bound of time delay $\tilde{\eta}$, and the minimum $\mathcal{H}_\infty$ performance index are discussed in detail.
b) As the first attempt, an FTCS is developed for the LFC, which can improve the reliability of the system. Besides, by considering the phenomenon of network congestion, the ETCS is applied into PSs to filter the transmitted signals for saving bandwidth resources.
c) Compared with the existing result for the SOFC problem in [34], which requires the system parameter matrix $\tilde{B}$ with the column full rank or the output matrix $\tilde{C}$ with the row full rank, the limitation is relaxed through the proposed method in this article. Furthermore, low conservative results are obtained by employing an improved inequality technology and the free-weighting matrix method.

The notations employed in this article can refer to [35], and some special cases are shown in Table I.

II. PROBLEM FORMULATION

A representative multiarea PSs model under the LFC scheme is exploited while considering the communication efficiency as well as the actuator faults in this section. In Section II-A, a model of LFC for multi-area PSs is presented. In Section II-B, an ETCS is presented to relieve the transmission of redundant packets. In Section II-C, based on the ETCS, the FTCS for multiarea PSs is established.

A. Model of LFC for Multiarea PSs

This section elaborates a dynamic model of ith control area in multiarea PSs, in which two communication channels are utilized for connecting the distributed control area to ensure the flexibility of the communication. The ith control area of the multiarea PSs is shown in Fig. 1, and the meaning of the corresponding parameters are given in Table I

$$\begin{cases} \dot{x}(t) = \tilde{A}x(t) + \tilde{B}u(t) + \tilde{F}\omega(t) \\ y(t) = \tilde{C}x(t) \end{cases} \tag{1}$$

where

$$\begin{aligned}
\tilde{A} &\triangleq \left[\tilde{A}_{ij}\right]_{n\times n}, x_i(t) \triangleq \left[x_{1i}(t)\ x_{2i}(t)\right]^T \\
\tilde{B} &\triangleq \text{diag}\left\{\tilde{B}_1\ \tilde{B}_2\ \ldots\ \tilde{B}_n\right\} \\
x_{1i}(t) &\triangleq \left[\triangle f_i(t)\ \triangle P_{\text{tie-i}}(t)\ \triangle P_{mi}(t)\right] \\
x(t) &\triangleq \left[x_1(t)\ \ldots\ x_n(t)\right]^T \\
y(t) &\triangleq \left[y_1(t)\ \ldots\ y_n(t)\right]^T \\
u(t) &\triangleq \left[u_1(t)\ \ldots\ u_n(t)\right]^T \\
x_{2i}(t) &\triangleq \left[\triangle P_{vi}(t)\ \int \text{ACE}_i(t)\right] \\
y_i(t) &\triangleq \left[\text{ACE}_i(t)\ \int \text{ACE}_i(t)\right]^T \\
\tilde{C} &\triangleq \text{diag}\left\{\tilde{C}_1\ \ldots\ \tilde{C}_n\right\} \\
\tilde{F} &\triangleq \text{diag}\left\{\tilde{F}_1\ \ldots\ \tilde{F}_n\right\} \\
\omega(t) &\triangleq \left[\triangle P_{d1}(t)\ \ldots\ \triangle P_{dn}(t)\right]^T
\end{aligned}$$

with

$$\tilde{A}_{ii} \triangleq \begin{bmatrix} \breve{A}_{ii} & 0 \\ \breve{C}_i & 0 \end{bmatrix}, \tilde{A}_{ij} \triangleq \begin{bmatrix} \breve{A}_{ij} & 0 \\ 0 & 0 \end{bmatrix}, \tilde{B}_i \triangleq \begin{bmatrix} \breve{B}_i \\ 0 \end{bmatrix}$$

$$\tilde{C}_i \triangleq \begin{bmatrix} \breve{C}_i & 0 \\ 0 & 1 \end{bmatrix}, \tilde{F}_i \triangleq \begin{bmatrix} \breve{F}_i \\ 0 \end{bmatrix}, \breve{A}_{ii} \triangleq \begin{bmatrix} \breve{A}_{1i} & \breve{A}_{2i} \\ \breve{A}_{3i} & \breve{A}_{4i} \end{bmatrix}$$

$$\breve{B}_i \triangleq \begin{bmatrix} 0 \\ 0 \\ 0 \\ \frac{1}{T_{gi}} \end{bmatrix}, \breve{F}_i \triangleq \begin{bmatrix} -\frac{1}{M_i} \\ 0 \\ 0 \\ 0 \end{bmatrix}, \breve{C}_i \triangleq \begin{bmatrix} \beta_i \\ 1 \\ 0 \\ 0 \end{bmatrix}^T$$

$$\breve{A}_{4i} \triangleq \begin{bmatrix} -\frac{1}{T_{\text{chi}}} & \frac{1}{T_{\text{chi}}} \\ 0 & -\frac{1}{T_{gi}} \end{bmatrix}, \breve{A}_{3i} \triangleq \begin{bmatrix} 0 & 0 \\ -\frac{1}{R_i T_{gi}} & 0 \end{bmatrix}$$

$$\breve{A}_{1i} \triangleq \begin{bmatrix} -\frac{D_i}{M_i} & -\frac{1}{M_i} \\ T & 0 \end{bmatrix}, \breve{A}_{2i} \triangleq \begin{bmatrix} \frac{1}{M_i} & 0 \\ 0 & 0 \end{bmatrix}$$

$$\breve{A}_{ij} \triangleq [(2,1) = 2\pi T_{ij}], T \triangleq 2\pi \sum\nolimits_{j=1, j\neq i}^{n} T_{ij}.$$

The meaning of $\text{ACE}_i(t)$ is the ith area control error (ACE). $x(t)$ represents the state vector. $y(t)$ is the output of the system. $\tilde{A}$,$\tilde{B}$, $\tilde{C}$, and $\tilde{F}$ are parameter matrices of the system. Now, we design the LFC with consideration of the communication network from the ACE to the controller. The PI controller can be established as follows [7]:

$$u_i(t) = -K_{Pi}\text{ACE}_i(t) - K_{Ii}\int \text{ACE}_i(t) \tag{2}$$

where K_{Pi} is the proportional gain and K_{Ii} is the integral gain.

Remark 1: While analyzing the LFC problem of the PSs, the main objective is to adjust the frequency deviation of the system to zero in a short time. Hence, the PI controller is appropriate for disposing of such a problem due to its quick response and none steady-state error. The frequency deviation can be adjusted to zero via employing the PI controller, and the transient response is enhanced contemporaneously. On account of the above-mentioned description, the PI controller is utilized to settle the LFC problem of the PSs extensively [36], [37].

B. Event-Triggered Communication Scheme

An ETCS is proposed in this section, which aims to acquire the satisfying control performance for alleviating the pressure of the communication channel. Fig. 1 illustrates the diagram of LFC for multiarea PSs under the ETCS. Then, a brief description of the LFC method is given as follows. First, the governor senses the frequent deviation $\triangle f_i(t)$ and then adjusts the positional deviation of $\triangle P_{vi}(t)$. After adjusting the positional deviation of the valve, the input steam entering the turbine is varied so that the mechanical output deviation for the generator $\triangle P_{mi}(t)$ is controlled, which results in a constant frequency. Nevertheless, as the main unit of the composition frequency control, the governor and the turbine cannot maintain the norm value by themselves. Therefore, the PI controller is considered in this article, which is necessary to adjust ACE for the turbine. It can make that the mechanical output deviation for the generator $\triangle P_{mi}(t)$ tracks the load changes disturbance deviation for the load $\triangle P_{di}(t)$, and restores the system frequency. After that, the controlled output with a zero-order holder (ZOH) is described as follows:

$$y(t) = \tilde{C}x(t_k) \tag{3}$$

where $x(t_k) \in R^m$ is the measured output and t_k is the moment of the transmitted sampling. The event-trigger in this article

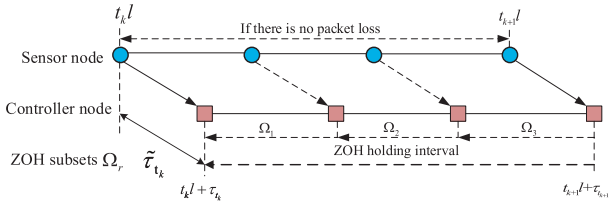

Fig. 2. Schematic of ZOH subsets.

consists of two parts. The first part is the information stored in registers on the newly released packet $(t_k, y(t_k l))$, another is a comparator which detects that whether the current SD packet $(t_k + r, y(t_k l + rl))$ satisfies the condition as below or not, where $t_{k+1} l$ is the moment in the future transmitted sampling instant determined by the ETCS as follows:

$$[y(i_k l) - y(t_k l)]^T \upsilon [y(i_k l) - y(t_k l)] \leq \alpha y^T(t_k l)\upsilon y(t_k l) \tag{4}$$

in which $\upsilon > 0$ is a weighting matrix, $i_k l = t_k l + rl, r \in N$, $t_k (k = 0, 1, 2, \ldots)$; l is the sampling period, and $\alpha > 0$ is a presupposed constant. $y(i_k l)$ is sent to the ZOH immediately through the communication network when condition (4) is violated; otherwise, drop it right away. Hence, as the instant in the next transmitted sampling instant, $t_{k+1} l$ is determined by the ETCS as follows:

$$t_{k+1} l = t_k l + \min_{l \in N}\{rl \mid \tilde{y}^T(i_k l)\upsilon \tilde{y}(i_k l) > \alpha y^T(t_k l)\upsilon y(t_k l)\}$$

where $\tilde{y}(i_k l) = y(i_k l) - y(t_k l)$.

Combining conditions (3) and (4), one has

$$t_{k+1} l = t_k l + \min_{l \in N}\left\{rl \mid e^T(i_k l)\Phi e(i_k l) > \alpha x^T(t_k l)\Phi x(t_k l)\right\} \tag{5}$$

where $e(i_k l) = x(i_k l) - x(t_k l)$, $\Phi = \tilde{C}^T \upsilon \tilde{C}$.

Remark 2: It should be noted that the Zeno phenomenon may occur in ETCS. From the communication point of view, if the communication channel under the ETCS has Zeno phenomenon during the communication, the event-trigger is triggered infinitely. Therefore, it is particularly important to set a sampling interval in the data transmission. According to condition (5), we set l to be a sampling period, which can effectively avoid the Zeno phenomenon.

If condition (5) is guaranteed, the SD is transmitted via the communication network channel when condition (5) is guaranteed, which saves more network bandwidth than the normal time-trigger scheme. In order to enable the above-mentioned communication scheme availing at each sampling moment, which judges the sampling data currently transmitted on the communication network can be discarded or not, we separate the holding interval $\Omega = [t_k l + \tilde{\tau}_{t_k}, t_{k+1} l + \tilde{\tau}_{t_{k+1}})$ of the ZOH into the following subsets Ω_r and Fig. 2 illustrates the subsets of ZOH

$$\Omega = \cup \Omega_r, \Omega_r = [i_r l + \tilde{\tau}_{t_k}, i_r l + l + \tilde{\varsigma}_{ir})$$

with $r = 0, 1, \ldots, t_{k+1} - t_k - 1$ and

$$\tilde{\varsigma}_{i_r} = \begin{cases} \tilde{\tau}_{t_k}, r = 0, 1, \ldots, t_{k+1} - t_k - 2 \\ \tilde{\tau}_{t_k+1}, r = t_{k+1} - t_k - 1. \end{cases}$$

Define $\eta(t) \triangleq t - i_r l,\ t \in \Omega_r$, and $\dot{\eta}(t) = 1, 0 \le \tilde{\tau}_{t_k} \le \eta(t) \le l + \tilde{\varsigma}_{ir} \le \tilde{\eta} = l + \tilde{\tau}_M$. Then, Controller (2) can be rewritten as the following form:

$$u_i(t) = K_i \tilde{C}_i x(t - \eta(t)) - K_i \tilde{C}_i e(i_r l), t \in \Omega_r. \tag{6}$$

Remark 3: If the communication delay $\tilde{\tau}_{t_k} \ge l$, it seems that the network still transmits the SD $y(t_k l)$, but the event generator has accepted the SD $y(t_k l + l)$. It may result in disarrangement in updating instants for obtaining the data. Therefore, we assume $\tilde{\tau}_M < l$ to avoid the aforementioned phenomenon.

C. Fault-Tolerant Multiarea LFC Model With Communication Networks

Noted that the actuator faults may occur in PSs because of the component aging, environmental factors, and so on. Therefore, designing a controller that can tolerate the occurrence of such faults is of great importance. Based on this inspiration, we derive the actuator faults model from [38]. The control input $u_f(t)$ is a signal transmitted from the actuator and obeys

$$u_f(t) = \tilde{\mathcal{F}} u(t) \tag{7}$$

in which

$$\tilde{\mathcal{F}} = \text{diag}\left\{f^1, f^2, \ldots, f^n\right\}$$

is the actuator faults matrix with known constants f_-^l, f_+^l and satisfying $0 \le f_-^l \le f^l \le f_+^l \le 1, l = 1, 2, \ldots, n$

Set

$$f_0^l = \frac{f_-^l + f_+^l}{2}, m^l = \frac{f^l - f_0^l}{2}, j^l = \frac{f_+^l - f_-^l}{f_+^l + f_-^l}. \tag{8}$$

Then, it is clear that

$$\tilde{\mathcal{F}} = \tilde{\mathcal{F}}_0 \left(I + \mathcal{M}\right), |\mathcal{M}| \le J \le I \tag{9}$$

where

$$|\mathcal{M}| \triangleq \text{diag}\left\{\left|m^1\right|, \left|m^2\right|, \ldots, \left|m^n\right|\right\}$$

$$\tilde{\mathcal{F}}_0 \triangleq \text{diag}\left\{f_0^1, f_0^2, \ldots, f_0^n\right\}, J \triangleq \text{diag}\left\{j^0, j^1, \ldots, j^n\right\}.$$

Remark 4: It is worth pointing that if the value of f^l changes, the operating mode of the corresponding actuator is also changed, which is not taken into account in [39] and [40]. More details can be described as follows:

1) the operating mode of the actuator is fault completely when $f^l = 0$;
2) under the condition that the range of f^l is between 0 and 1, the operating mode of the actuator is the partial fault;
3) when $f^l = 1$, the operating mode of the actuator is normal.

According to formulas (1), (6), and (7), model (1) can be expounded as

$$\begin{cases} \dot{x}(t) = \tilde{A}x(t) - \tilde{B}\tilde{\mathcal{F}}K\tilde{C}x(t - \eta(t)) \\ \quad +\tilde{B}\tilde{\mathcal{F}}K\tilde{C}e(i_r h) + \tilde{F}\omega(t) \\ y(t) = \tilde{C}x(t), t \in \Omega_r. \end{cases} \tag{10}$$

Remark 5: For a detailed time series analysis, we divided the holding interval of the ZOH $t \in \Omega$ into sampling-interval-like subsets $\Omega_r = [i_k l + \tilde{\tau}_{t_k}, i_k l + l + \tilde{\varsigma}_{ir})$, i.e., $\Omega = \cup\Omega_r$, where

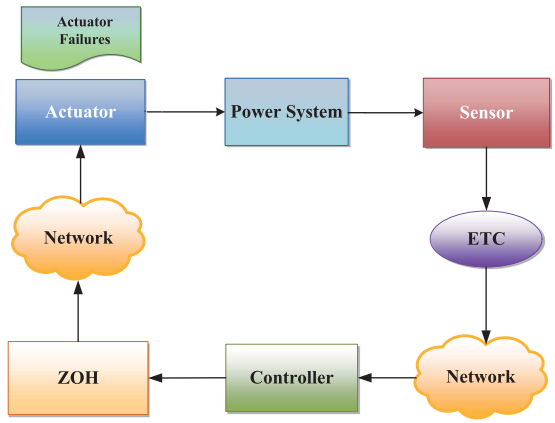

Fig. 3. Framework of an event-triggered fault-tolerant strategy for multiarea PSs.

$i_k l = t_k l + rl,\ r = 0, \ldots, t_{k+1} - t_k - 1$ means the sampling instants from the current transmitted sampling instant $t_k l$ to the future transmitted sampling instant $t_{k+1} l$. One has $\tilde{\tau}_{i_k+1} = \tilde{\tau}_{t_{k+1}}$ under the condition that r takes the value as $t_{k+1} - t_k - 1$, otherwise, $\tilde{\tau}_{i_k+1} = \tilde{\tau}_{t_k}$. See Fig. 2 for illustration.

The purpose of this article is to analyze the multiarea PSs (10) under the ETCS and the FTCS, whose framework is shown in Fig. 3 and guarantee the following:

1) system (10) with $\omega(t) \equiv 0$ is asymptotically stable;
2) for the nonzero $\omega(t) \in L_2[0, \infty)$, an $\mathcal{H}_\infty$ performance is guaranteed, that is, under the zero initial conditions, the inequality $\int_0^{+\infty} y^T(t) y(t) dt \le \mu^2 \int_0^{+\infty} \omega^T(t) \omega(t) dt$ holds, in which $\mu > 0$ is a pregiven constant.

Remark 6: The researched system with the ETCS, the FTCS and an LFC is established as an ACE-based system (10) with time-varying delay $\eta(t)$, which is structured by a sawtooth function. As the closed-loop system (10) relies on $x(t - \eta(t))$ and $e(i_r l)$ simultaneously, meanwhile, considering the possible actuator failure in the operation, it is convenient for us to employ the presented ETCS and FTCS to analyze and synthesize the multiarea PSs.

III. Main Results

First, the stability criteria for multiarea PSs (10) under ETCS and the FTCS are deduced in this section. Then, on account of the raised method in fault-tolerant event-triggered LFC, the corresponding controller gains and the optimal $\mathcal{H}_\infty$ performance index can be acquired. For simplifying notations, we define that

$$\vartheta_1 \triangleq \frac{1}{\eta(t)} \int_{t-\eta(t)}^{t} x(s) ds$$

$$\vartheta_2 \triangleq \frac{1}{\tilde{\eta} - \eta(t)} \int_{t-\tilde{\eta}}^{t-\eta(t)} x(s) ds$$

$$e_a \triangleq \left[0_{n,(a-1)n}\ I_n\ 0_{n,(5-1)n}\right]$$

$$(a = 1, 2, \ldots, 5)$$

$$\Xi = \begin{bmatrix} \text{diag}\{-Z, -3Z\} & S \\ * & \text{diag}\{-Z, -3Z\} \end{bmatrix}$$

$$\tilde{\psi}(t) \triangleq \left[\tilde{\psi}_1^T(t)\ \tilde{\psi}_2^T(t)\ \tilde{\psi}_3^T(t)\right]^T$$
$$\tilde{\psi}_3(t) \triangleq \left[\tilde{C}^T e^T(i_l h)\ \omega^T(t)\right]^T$$
$$\tilde{\psi}_2(t) \triangleq \begin{bmatrix}\vartheta_1^T \\ \vartheta_2^T\end{bmatrix}, \Upsilon(t) \triangleq \begin{bmatrix}\Theta(t) \\ \Psi(t)\end{bmatrix}$$
$$\tilde{\psi}_1(t) \triangleq \left[x^T(t)\ x^T(t-\eta(t))\ x^T(t-\tilde{\eta})\right]^T$$
$$\Theta(t) \triangleq \begin{bmatrix}x\left(t-\eta(t)\right)-x(t) \\ x\left(t-\eta(t)\right)+x(t)-2\vartheta_1\end{bmatrix}$$
$$\Psi(t) \triangleq \begin{bmatrix}x\left(t-\tilde{\eta}\right)-x\left(t-\eta(t)\right) \\ x\left(t-\tilde{\eta}\right)+x\left(t-\eta(t)\right)-2\vartheta_2\end{bmatrix}.$$

Theorem 1: For system (10) and a scalar $\tilde{\eta} > 0$, if there exist symmetric matrices $S \triangleq \left[\begin{smallmatrix}S_{11} & S_{12} \\ S_{13} & S_{22}\end{smallmatrix}\right] > 0,\ P > 0,\ Q > 0,\ \mathcal{Z} \triangleq \text{diag}\{Z, 3Z\} > 0,\ W > 0$, satisfying the following inequalities

$$\sum_{i=1}^{8} \Lambda_i < 0 \tag{11}$$
$$\begin{bmatrix}\mathcal{Z} & S \\ * & \mathcal{Z}\end{bmatrix} > 0 \tag{12}$$

where

$$\Lambda_1 \triangleq \text{sym}\{e_1^T P A e_1 + e_1^T P F e_7\} + e_1^T Q e_1 - e_3^T Q e_3$$
$$\Lambda_2 \triangleq \Upsilon^T(t)\Xi\Upsilon(t) + e_2^T \alpha\phi W e_2 - e_6^T \upsilon e_6$$
$$\Lambda_3 \triangleq \text{sym}\{e_1^T \frac{\pi^2}{4} W e_2\} - e_1^T \frac{\pi^2}{4} W e_1 - e_2^T \frac{\pi^2}{4} W e_2$$
$$\Lambda_4 \triangleq e_1^T \tilde{\eta} \tilde{A}^T Z e_8 + e_7^T \tilde{\eta} F^T Z e_8 - e_8^T \tilde{\eta} Z e_8$$
$$\Lambda_5 \triangleq e_1^T \tilde{\eta} \tilde{A}^T W e_9 + e_7^T \tilde{\eta} F^T W e_9 - e_9^T \tilde{\eta} W e_9$$
$$\Lambda_6 \triangleq e_1^T \tilde{C}^T e_{10} - e_{10} I e_{10} - e_7^T \mu^2 e_7$$
$$\Lambda_7 \triangleq \text{sym}\{e_1^T P \tilde{B} F_0 (I + M) K (e_6 - \tilde{C} e_2)\}$$
$$\Lambda_8 \triangleq (e_6^T - e_2^T \tilde{C}^T)[\tilde{\eta} \tilde{B} F_0 (I + M) K]^T (Z^T e_8 + W^T e_9)$$

then the asymptotic stability of system (10) with the $\mathcal{H}_\infty$ performance index μ is guaranteed by the ETC controller (6).

Proof 1: See Appendix A.

After a series of derivation and transformation to inequalities, a sufficient condition ensuring the asymptotic stability of system (10) with an $\mathcal{H}_\infty$ performance is obtained. But some unknown matrices coupling terms still exists in Theorem 1, which is arduous to obtain the desired gains. To this end, we employ a new method to obtain the desired controller gains, and it is presented as follows.

Theorem 2: For system (10) and a scalar $\tilde{\eta} > 0$, if there exist symmetric matrices $S \triangleq \left[\begin{smallmatrix}S_{11} & S_{12} \\ S_{13} & S_{22}\end{smallmatrix}\right] > 0,\ P > 0,\ Q > 0,\ \mathcal{Z} \triangleq \text{diag}\{Z, 3Z\} > 0,\ W > 0,\ \varepsilon_i > 0\ (i = 1, 2, \ldots, 6)$, and matrices T, U, satisfying condition (12)

$$\sum_{i=1}^{5} \tilde{\Lambda}_i + \sum_{i=1}^{6} \Lambda_i < 0 \tag{13}$$

where

$$\tilde{\Lambda}_1 \triangleq \text{sym}\{e_1^T \tilde{B} U (e_6 - \tilde{C} e_2)\}$$
$$\digamma_1 \triangleq e_6 - e_2 C^T, \digamma_2 \triangleq e_{12} + d(e_{13} + e_{15})$$
$$\digamma_3 \triangleq e_{18} + d(e_{22} + e_{20}), \tilde{\Lambda}_2 \triangleq \digamma_1^T U^T \tilde{B}^T (e_8 + e_9)$$
$$\tilde{\Lambda}_5 \triangleq (e_6^T - e_2^T \tilde{C}^T)(U^T \digamma_2 + K^T \digamma_3) \tag{14}$$
$$\begin{aligned}\tilde{\Lambda}_3 \triangleq\ & e_1^T[\left(P\tilde{B}F_0 - ST\right) e_{11} + P\tilde{B}F_0 e_{17}] \\ & + e_8^T[(Z\tilde{B}F_0 - GT)e_{14} + Z\tilde{B}F_0 e_{19}] \\ & + e_9^T[(W\tilde{B}F_0 - VT)e_{16} + W\tilde{B}F_0 e_{21}]\end{aligned}$$
$$\begin{aligned}\tilde{\Lambda}_4 \triangleq\ & - e_{11}^T \varepsilon_1^{-1} e_{11} - e_{12}^T \varepsilon_1 e_{12} - e_{13}^T \varepsilon_2^{-1} e_{13} - e_{14}^T \varepsilon_2 e_{14} \\ & - e_{15}^T \varepsilon_3^{-1} e_{15} - e_{16}^T \varepsilon_3 e_{16} - e_{17}^T \varepsilon_4^{-1} e_{17} - e_{18}^T \varepsilon_4 e_{18} \\ & - e_{19}^T \varepsilon_5^{-1} e_{19} - e_{20}^T \varepsilon_5 e_{20} - e_{21}^T \varepsilon_6^{-1} e_{21} - e_{22}^T \varepsilon_6 e_{22}\end{aligned} \tag{15}$$

then system (10) is asymptotically stable, which is guaranteed by the FETS controller (6) with the $\mathcal{H}_\infty$ performance index μ, and the corresponding gains matrix $K = T^{-1}U$.

Proof 2: See Appendix B.

Remark 7: For disposing of the coupling terms $P\tilde{B}F_0K$, $Z\tilde{B}F_0K$, and $W\tilde{B}F_0K$, we introduce some auxiliary matrices S, G, and V, which transmit the term $P\tilde{B}F_0K$, $Z\tilde{B}F_0K$, and $W\tilde{B}F_0K$ as $(P\tilde{B}F_0 - ST)T^{-1}U + SU$, $(Z\tilde{B}F_0 - GT)T^{-1}U + GU$ and $(W\tilde{B}F_0 - VT)T^{-1}U + VU$. This method can remove some limitations in [34] such as stipulating the system parameter matrix $\tilde{B}$ with the column full rank form or the output matrix $\tilde{C}$ with the row full rank form. Hence, this method is more general than the one in [34].

Theorem 3: For system (10) and a scalar $\tilde{\eta} > 0$, if there exist symmetric matrices $S \triangleq \left[\begin{smallmatrix}S_{11} & S_{12} \\ S_{13} & S_{22}\end{smallmatrix}\right] > 0,\ P > 0,\ Q > 0,\ \mathcal{Z} \triangleq \text{diag}\{Z, 3Z\} > 0,\ W > 0,\ \varepsilon_q, \tilde{\varepsilon}_q > 0,\ (q = 1, 2, \ldots, 6)$, and matrices $T,\ U$, satisfying condition (12) and following conditions

$$\breve{\Lambda} < 0 \tag{16}$$

where

$$\breve{\Lambda} \triangleq \sum_{i=1}^{3} \tilde{\Lambda}_i + \sum_{i=1}^{6} \Lambda_i + \breve{\Lambda}_4 + \breve{\Lambda}_5$$
$$\breve{\Lambda}_5 \triangleq (e_6^T - e_2^T \tilde{C}^T) U^T (\digamma_2 + \digamma_3)$$
$$\begin{aligned}\breve{\Lambda}_4 \triangleq\ & - e_{12}^T \varepsilon_1 e_{12} - e_{13}^T \varepsilon_2 e_{13} - e_{15}^T \varepsilon_3 e_{15} - e_{17}^T \varepsilon_4 e_{17} \\ & - e_{19}^T \varepsilon_5 e_{19} - e_{21}^T \varepsilon_6 e_{21} - e_{11}^T (\varepsilon_1 - \text{sym}\{T\}) e_{11} \\ & - e_{14}^T (\varepsilon_2 - \text{sym}\{T\}) e_{14} - e_{16}^T (\varepsilon_3 - \text{sym}\{T\}) e_{16}\end{aligned}$$

TABLE II
PARAMETERS OF THREE-AREA LFC STRATEGY

parameter	R	D	β	$M(s)$	$T_{chi}(s)$	$T_g(s)$
$Area1$	0.05	1.0	21.0	10	0.3	0.1
$Area2$	0.05	1.5	21.5	12	0.4	0.17
$Area3$	0.05	1.8	21.8	12	0.35	0.20
T_{12} = 0.1986, T_{13} = 0.2148, T_{23} = 0.1830						

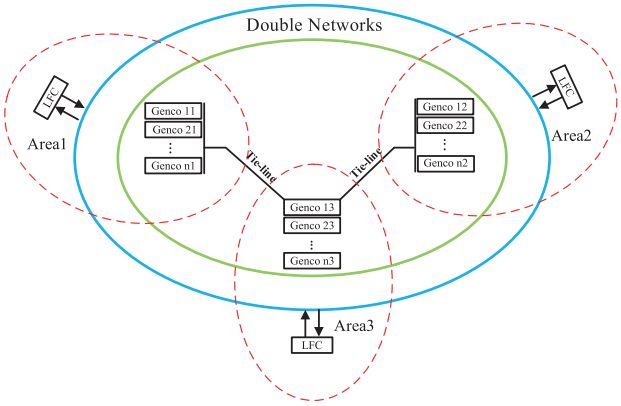

Fig. 4. Schematic for a three-area interconnected PSs.

$$- e_{18}^T(\varepsilon_4 - \text{sym}\{T\})e_{18} - e_{20}^T(\varepsilon_5 - \text{sym}\{T\})e_{20}$$
$$- e_{22}^T(\varepsilon_6 - \text{sym}\{T\})e_{22}$$

then system (10) is asymptotically stable with an $\mathcal{H}_\infty$ performance index μ, and the corresponding gain matrix can be solved by $K = T^{-1}U$.

Proof 3: Define

$$U \triangleq TK, \mathring{\mathcal{G}}_1 = \text{diag}\left[I_{17\times 17}, T, I, T, I, T\right].$$

By pre- and postmultiplying condition (13) with $\mathring{\mathcal{G}}_1^T$ and $\mathring{\mathcal{G}}_1$, and according to the inequality

$$-T\varepsilon^{-1}T^T \leq \varepsilon - \text{sym}\{T\}$$

conditions (12) and (16) can be established naturally.

Remark 8: The ETCS for the LFC with communication delay is derived from Lebesgue sampling (LS) [12], which results in the ETCS hindering to exploit because of its characteristics including aperiodicity, non-Gaussian and nonlinearity. Furthermore, as an event function, the probability of the event occurring in LS is uncertain. Hence, when analyzing the system with the fault-tolerant event-triggered strategy (FTETS), we need to treat it as a hybrid nonlinear system.

IV. SIMULATION

This section expounds on the research of three-area PSs interconnected via two communication channels to illustrate the validity of the method in this article. For achieving the objective of analyzing the stability in the system, corresponding required parameters defined in formula (10) are stated in Table II. Fig. 4 illustrates the schematic of the three-area interconnected PSs enlightened by [41], where Areas 1, 2, and 3 express PSs with the LFC strategy, and their corresponding communication channels are represented by the arrow lines. The blue line and green line represent the primary channel and standby channel, respectively. Meanwhile, the system performance may be deteriorated by the time delay, which may lead to the instability of the PSs. And the corresponding instability of the LFC strategy expresses the declination far away from 0, which consists in the frequency and ACE.

Remark 9: The double communication channel mentioned in this article is a kind of SDH optic fiber network. It has many structures, such as chain, star, ring, and network port. Among them, the double communication channel, which is also named as a dual-ring structure, is a common form. It is widely used because it has a self-healing function and can provide high reliability. It is composed of two links forming two rings, one as the primary ring and another as the backup ring. Data is transmitted on both links at the same time, and only data from the primary link is accepted under normal conditions. Data from the backup link starts to be accepted within 50 ms when the primary link is under failure.

By solving the linear matrix inequalities in Theorem 3 with the upper bound delay $\tilde{\eta} = 0.1, \alpha = 0.1$, performance parameter $\mu = 25$, the corresponding controller gain can be obtained

$$K = \text{diag}\{K_1, K_2, K_3\}$$
$$K_1 = \left[-0.0114\ -0.6841\right]$$
$$K_2 = \left[-0.0062\ -0.5166\right]$$
$$K_3 = \left[-0.0080\ -0.6129\right].$$

For the PSs controlled by the FTETS under the LFC scheme with the largest sampled interval, the minimum value of the $\mathcal{H}_\infty$ performance index μ can be acquired via the Algorithm 1.

Table III shows the relationship between the triggering parameter α and the time delay upper bound $\tilde{\eta}$. According to the information from Table III, the larger α is, the larger $\tilde{\eta}$ is. It originates from the fact that the larger α may result in the larger residence time of the sample, which causes the system performance to decrease. And the time delay $\tilde{\eta}$ increases at this time.

Remark 10: Enhancing the sampling interval will reduce the frequency of the data transmission, which can relieve the communication burden. However, the system with an overlarge sampling interval may lose some useful information and distort part of the received data, which can reduce the performance of the system. Hence, the sampling interval of the system is interrelated with the system performance.

According to the information shown in Table IV, the following results can be obtained. As the maximum sampling interval $\tilde{\eta}$ decreases while the parameter α holds invariant, $\mu_{\min}$ decreases continuously, where Remark 10 elaborates the relationship between the sampling interval $\tilde{\eta}$ and the optimal $\mathcal{H}_\infty$ performance index $\mu_{\min}$. Note that the system performance rises rapidly when the sampling interval decreases from 0.2 to 0.15, and the rising variation of the system performance is lower than the previous change while the sampling interval decreases from 0.1 to 0.05. The information aforementioned strongly proves that choosing a suitable sampling interval has a profound influence

Algorithm 1: The Minimum Value of μ.

Require: Given the system parameters and corresponding scalars α, $\tilde{\eta}$, the $\Delta\mu$ is selected as the accuracy and its upper bound value is μ_{end}, and let the initial value $\mu_{start} = 0$

Ensure: The optimal performance index $\mu_{\min}$

1: **if** In Theorem 3, the conditions are valuable with μ_{end} **then** pass to 5;
2: **else** let $\mu_{end} = 2 * \mu_{end}$;
3: **end if**
4: Solve the LMIs in Theorem 3 by setting $\mu = \frac{\mu_{start}+\mu_{end}}{2}$;
5: **if** $|\mu_{end} - \mu| > \Delta\mu$ **then**
6: **if** the conditions are valuable with μ in Theorem 3 **then** $\mu = \mu_{end}$, and return to 5;
7: **else** $\mu = \mu_{start}$, and return to 5;
8: **end if**
9: **else**
10: **if** the conditions are valuable with μ in Theorem 2 **then** $\mu_{\min} = \mu$;
11: **else** $\mu_{\min} = \mu_{end}$ and return to 6;
12: **end if**
13: **end if**
14: **Return** $\mu_{\min}$

TABLE III
UPPER BOUNDS OF DELAY $\tilde{\eta}$ DERIVED FOR DIFFERENT α

α	0.1	0.2	0.3	0.4	0.5
$\tilde{\eta}$	0.7567	0.7569	0.7571	0.7577	0.7583

TABLE IV
RELATIONSHIP AMONG BOUNDS OF DELAY $\tilde{\eta}$, TRIGGERING PARAMETER ϱ, AND MINIMUM VALUE OF $\mu_{\min}$

$\mu_{\min}$	$\tilde{\eta} = 0.2$	$\tilde{\eta} = 0.15$	$\tilde{\eta} = 0.1$	$\tilde{\eta} = 0.05$
$\alpha = 0.1$	1.4239	1.0914	0.6558	0.3058
$\alpha = 0.2$	1.4166	1.0215	0.6487	0.2978
$\alpha = 0.3$	1.4133	1.0203	0.6455	0.2931

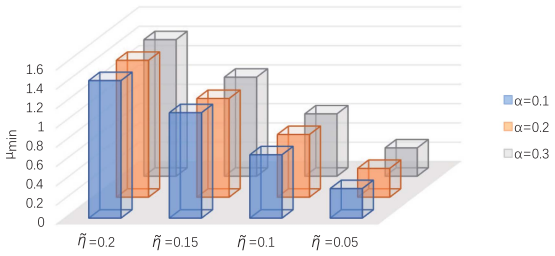

Fig. 5. Graph of the relationship among $\tilde{\eta}$, α, and $\mu_{\min}$.

on the system performance. Furthermore, as the parameter α increases while sampling interval $\tilde{\eta}$ remains invariant, the value of $\mu_{\min}$ also increases continuously, which illustrates the system performance deteriorates with the increases of α. However, from Fig. 5, the parameter α has little impact on the system performance.

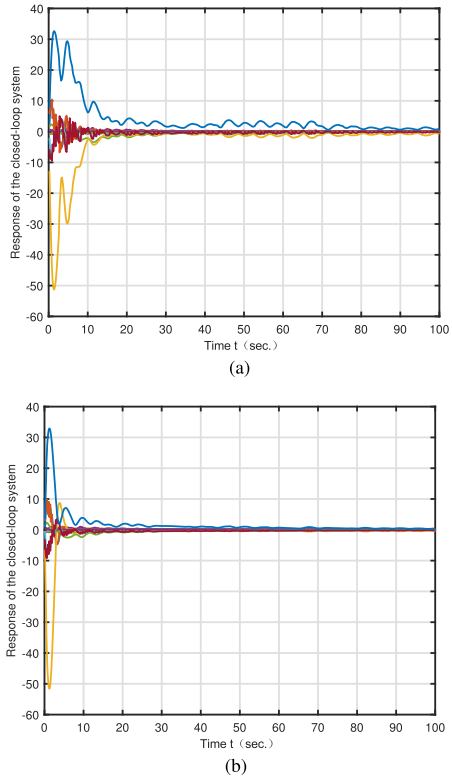

Fig. 6. Comparison of the state responses corresponding to the gain obtained with and without failure. (a) State responses corresponding to the gain obtained without failure. (b) State responses corresponding to the gain obtained with failure.

For better illustrating the necessity by utilizing the FTCS in this article, a comparison of the state responses corresponding to the gain obtained with and without failure is given. By using above-mentioned parameters, the controller gain $\tilde{K}$ without actuator failure can be obtained as

$$\tilde{K} = \text{diag}\{\tilde{K}_1, \tilde{K}_2, \tilde{K}_3\}$$
$$\tilde{K}_1 = \begin{bmatrix} -0.0071 & -0.6073 \end{bmatrix}$$
$$\tilde{K}_2 = \begin{bmatrix} -0.0039 & -0.4213 \end{bmatrix}$$
$$\tilde{K}_3 = \begin{bmatrix} -0.0048 & -0.4896 \end{bmatrix}.$$

The main purpose is to find out the corresponding controller gain with and without actuator failure, respectively. The system is then analyzed by using two sets of gains under the actuator failure, and finally observes the change of the response of the system. The details are as follows: in the case of a system without actuator failure, the associated gain is solved as $\tilde{K}$, and the associated gain is solved as K in the case of a system with actuator failure, and finally, in the case of a system with actuator failure, the responses of the system are analyzed by using K $\tilde{K}$, respectively. First, setting $x_v(0) = 0(v = 1, \ldots, 15)$ as the initial value, the external disturbance $\omega(t) = [\ \frac{\sqrt{0.16}}{1+t^2}\ \frac{\sqrt{0.16}}{1+t^2}\ \frac{\sqrt{0.16}}{1+t^2}\ ]^T$, Fig. 6 can be acquired. Fig. 6 represents the comparison of the state responses corresponding to the gains obtained with

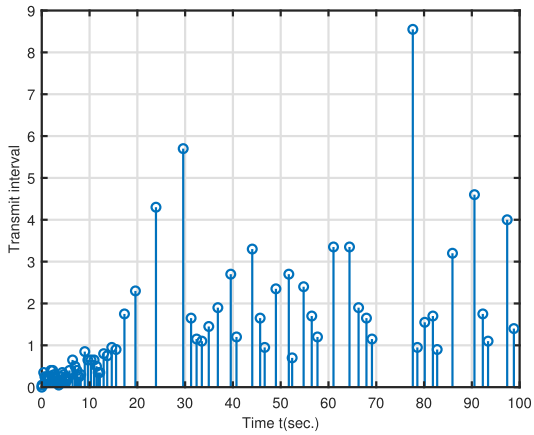

Fig. 7. Release intervals of ETC.

and without failure. Fig. 6(a) and (b), respectively, illustrates the state responses of the closed-loop system without and with actuator faults. By comparing two figures, it can be found that the state responses of the system corresponding to the controller gain obtained without failure in Fig. 6(a) jitter more frequently and, in addition, are still in the jittered state at 100 s. However, in Fig. 6(b), the state responses of the system corresponding to the controller gain obtained under actuator failure are smoother than Fig. 6(a) and, basically, converges to 0 at 60 s. Thus, the fault-tolerant controller designed in this article can, to a certain extent, alleviate the problems caused by actuator failure and enhance the reliability of the system. Fig. 7 is the release intervals of the ETCS. Each vertical line similar to a match stick expresses the moment of each triggering, and the length of the vertical line indicates the duration of saving data after the trigger. From Fig. 7, within $[0, 15]s$, the number of triggering is quite frequent with a short time to save data, which implies that the gaps among the data are large, and the system is unstable with the great state changes. However, compared with the time frame in $[0, 15]s$, the number of triggering is gradually decreasing within $[15, 100]s$. And its saving of the data is gradually getting longer, which illustrates the fact that the system state changes slowly and the system becomes stable gradually. To sum up, according to the comparison result in Fig. 6, and the release interval of ETCS in Fig. 7, the validity and reliability of the proposed method are demonstrated.

V. Conclusion

The $\mathcal{H}_\infty$ control problem for multiarea power systems via the LFC scheme has been considered in this work. For saving the constrained bandwidth resources, reducing the frequency of controller updating as well as handling the possible actuator failure during the operation of the system, the ETCS and FTCS have been adopted. Besides, some sufficient conditions which ensure the stability of power systems with an $\mathcal{H}_\infty$ performance index have been deduced while taking the limitation of network bandwidth resources and the system into account according to the established model as well as communication scheme. Finally, an explained example has been employed to illustrate the advantages of the proposed method. Since cyber-attacks can cause packets to be lost during the data transmission [42], which may seriously affect the accuracy of the system updating. How to integrate the cyber-attacks into the fault-tolerant event-triggered controller is fascinating, which motivates us to explore in the future.

Appendix

A. Proof of Theorem 1

For system (10), the following Lyapunov–Krasovskii functional can be selected:

$$V(t) = \sum\nolimits_{b=1}^{3} V_b(t) \tag{17}$$

in which

$$V_1(t) = x^T(t)Px(t) + \int_{t-\bar{\eta}}^{t} x^T(s)Qx(s)ds$$

$$V_2(t) = \tilde{\eta}\int_{-\bar{\eta}}^{0}\int_{t+\beta}^{t} \dot{x}^T(s)Z\dot{x}(s)dsd\beta$$

$$V_3(t) = \tilde{\eta}^2\int_{t-\eta(t)}^{t} \dot{x}^T(s)W\dot{x}(s)ds - \frac{\pi^2}{4}\int_{t-\eta(t)}^{t} \xi_1^T(s)W\xi_1(s)ds$$

with $\xi_1(s) = x(s) - x(t-\eta(s))$.

Then, the derivative of formula (17) along the trajectories of system (10) can be acquired

$$\begin{aligned}\dot{V}_1(t) &= \text{sym}\left\{x^T(t)P\dot{x}(t)\right\} + x^T(t)Qx(t) \\ &\quad - x\left(t-\tilde{\eta}\right)Qx\left(t-\tilde{\eta}\right) \\ &= \text{sym}\{x^T(t)P\tilde{A}x(t) - x^T(t)P\tilde{B}\tilde{\mathcal{F}}K\tilde{C}x(t-\eta(t)) \\ &\quad + x^T(t)P\tilde{B}\tilde{\mathcal{F}}K\tilde{C}e(i_l h) + x^T(t)PF\omega(t)\} \\ &\quad + x^T(t)Qx(t) - x\left(t-\tilde{\eta}\right)Qx\left(t-\tilde{\eta}\right) \\ &= \tilde{\psi}^T(t)[\text{sym}\{e_1^TP\tilde{A}e_1 - e_1^TP\tilde{B}\tilde{\mathcal{F}}_0\left(I+M\right)K\tilde{C}e_2 \\ &\quad + e_1^TP\tilde{B}\tilde{\mathcal{F}}_0\left(I+M\right)Ke_6 + e_1^TPFe_7\} \\ &\quad + e_1^TQe_1 - e_3^TQe_3]\tilde{\psi}(t)\end{aligned} \tag{18}$$

$$\dot{V}_2(t) = \tilde{\eta}^2\dot{x}^T(t)Z\dot{x}(t) - \tilde{\eta}\int_{t-\tilde{\eta}}^{t}\dot{x}^T(s)Z\dot{x}(s)ds \tag{19}$$

$$\begin{aligned}\dot{V}_3(t) &= \tilde{\eta}^2\dot{x}^T(t)W\dot{x}(t) - \frac{\pi^2}{4}[x^T(t) \\ &\quad - x^T\left(t-\eta(t)\right)]W\left[x(t) - x\left(t-\eta(t)\right)\right] \\ &= \tilde{\eta}^2\dot{x}^T(t)W\dot{x}(t) - \frac{\pi^2}{4}\tilde{\psi}^T(t)[e_1^T(t)We_1(t) \\ &\quad - \text{sym}\{e_1^T(t)We_2(t)\} + e_2^T(t)We_2(t)]\tilde{\psi}(t).\end{aligned} \tag{20}$$

Noted that $-\tilde{\eta}\int_{t-\tilde{\eta}}^{t}\dot{x}^T(s)Z\dot{x}(s)ds$ in $\dot{V}_2(t)$ can derive the following inequality, which is enlightened by the Wirtinger inequality [43] as well as the convex optimization technique [44]:

$$-\tilde{\eta}\int_{t-\tilde{\eta}}^{t}\dot{x}^T(s)Z\dot{x}(s)ds$$

$$
\begin{aligned}
&= -\tilde{\eta}\int_{t-\eta(t)}^{t}\dot{x}^T(s)Z\dot{x}(s)ds-\tilde{\eta}\int_{t-\tilde{\eta}}^{t-\eta(t)}\dot{x}^T(s)Z\dot{x}(s)ds\\
&\le -\frac{\tilde{\eta}}{\eta(t)}\Theta^T(t)Z\Theta(t)-\frac{\tilde{\eta}}{\tilde{\eta}-\eta(t)}\Psi^T(t)Z\Psi(t)\\
&\le \Upsilon^T(t)\Xi\Upsilon(t). \qquad (21)
\end{aligned}
$$

From conditions (5) and (18)–(21), the inequality can be obtained as follows:

$$\dot{V}(t)\le\tilde{\psi}^T(t)(\sum_{i=1}^{3}\Lambda_i+\Lambda_7)\tilde{\psi}(t)+\tilde{\eta}^2\dot{x}^T(s)(W+Z)\dot{x}(s).$$

According to the above-mentioned derivation, the following inequality can be obtained naturally:

$$
\begin{aligned}
&\dot{V}(t)+y^T(t)y(t)-\mu^2\omega^T(t)\omega(t)\\
&\quad\le\tilde{\psi}^T(t)\left[\sum_{i=1}^{3}\Lambda_i+\Lambda_6+\Lambda_7\right]\tilde{\psi}(t)\\
&\qquad+\tilde{\eta}^2\dot{x}^T(t)(W+Z)\dot{x}(t)\\
&\quad=\tilde{\psi}^T(t)\Lambda\tilde{\psi}(t).
\end{aligned}
$$

If conditions (11) and (12) hold, in the light of conditions (18)–(20), then

$$\dot{V}(t)+y^T(t)y(t)-\mu^2\omega^T(t)\omega(t)\le 0. \qquad (22)$$

Owing to $\dot{V}(t)$ being a continuous function, ones integrate from 0 to $+\infty$ on both sides of (22), then

$$
\begin{aligned}
V(+\infty)-V(0)+\int_0^{+\infty}y^T(t)y(t)dt\\
-\mu^2\int_0^{+\infty}\omega^T(t)\omega(t)dt<0.
\end{aligned}
$$

By virtue of $V(+\infty)\ge 0$ and $V(0)=0$, then

$$\int_0^{+\infty}y^T(t)y(t)dt-\mu^2\int_0^{+\infty}\omega^T(t)\omega(t)dt\le 0$$

which implies that system (10) guarantees the $\mathcal{H}_\infty$ performance index μ.

B. Proof of Theorem 2

Enlightened by Theorem 1

$$\Lambda=\sum_{i=1}^{6}\Lambda_i+\sum_{i=1}^{6}\varphi_i<0 \qquad (23)$$

where

$$
\begin{aligned}
\varphi_1&\triangleq\begin{bmatrix}0_{1\times1}&\iota_1\\ \iota_1^T&0_{9\times9}\end{bmatrix},\varphi_3\triangleq\begin{bmatrix}0_{7\times7}&\iota_3^T\\ \iota_3&0_{3\times3}\end{bmatrix}\\
\varphi_2&\triangleq\begin{bmatrix}0_{1\times1}&\iota_2\\ \iota_2^T&0_{9\times9}\end{bmatrix},\varphi_4\triangleq\begin{bmatrix}0_{7\times7}&\iota_4^T\\ \iota_4&0_{3\times3}\end{bmatrix}\\
\varphi_5&\triangleq\begin{bmatrix}0_{8\times8}&\iota_5^T\\ \iota_5&0_{2\times2}\end{bmatrix},\varphi_6\triangleq\begin{bmatrix}0_{8\times8}&\iota_6^T\\ \iota_6&0_{2\times2}\end{bmatrix}\\
\iota_1&\triangleq\begin{bmatrix}-P\tilde{B}F_0K\tilde{C}\ 0_{1\times3}\ P\tilde{B}F_0K\tilde{C}\ 0_{1\times4}\end{bmatrix}\\
\iota_2&\triangleq\begin{bmatrix}-P\tilde{B}F_0MK\tilde{C}\ 0_{1\times3}\ P\tilde{B}F_0MK\tilde{C}\ 0_{1\times4}\end{bmatrix}\\
\iota_3&\triangleq\begin{bmatrix}\tilde{\iota}_{31}\ \tilde{\iota}_{32}\end{bmatrix},\tilde{\iota}_{31}\triangleq\begin{bmatrix}0_{1\times1}&-\tilde{\eta}Z\tilde{B}F_0K\tilde{C}\\ 0_{2\times1}&0_{2\times1}\end{bmatrix}\\
\tilde{\iota}_{32}&\triangleq\begin{bmatrix}0_{1\times3}\ \tilde{\eta}Z\tilde{B}F_0K\tilde{C}\ 0_{1\times1}\\ 0_{2\times3}\quad 0_{2\times1}\quad 0_{2\times1}\end{bmatrix},\iota_4\triangleq\begin{bmatrix}\tilde{\iota}_{41}\ \tilde{\iota}_{42}\end{bmatrix}\\
\tilde{\iota}_{41}&\triangleq\begin{bmatrix}0_{1\times1}&-\tilde{\eta}Z\tilde{B}F_0MK\tilde{C}\\ 0_{2\times1}&0_{2\times1}\end{bmatrix},\iota_5\triangleq\begin{bmatrix}\tilde{\iota}_{51}\ \tilde{\iota}_{52}\end{bmatrix}\\
\tilde{\iota}_{42}&\triangleq\begin{bmatrix}0_{1\times3}\ \tilde{\eta}Z\tilde{B}F_0MK\tilde{C}\ 0_{1\times1}\\ 0_{2\times3}\quad 0_{2\times1}\quad 0_{2\times1}\end{bmatrix}\\
\tilde{\iota}_{51}&\triangleq\begin{bmatrix}0_{1\times1}&-\tilde{\eta}W\tilde{B}F_0K\tilde{C}\\ 0_{1\times1}&0_{1\times1}\end{bmatrix},\iota_6\triangleq\begin{bmatrix}\tilde{\iota}_{61}\ \tilde{\iota}_{62}\end{bmatrix}\\
\tilde{\iota}_{52}&\triangleq\begin{bmatrix}0_{1\times3}\ \tilde{\eta}W\tilde{B}F_0K\tilde{C}\ 0_{1\times1}\\ 0_{1\times3}\quad 0_{1\times1}\quad 0_{1\times1}\end{bmatrix}\\
\tilde{\iota}_{61}&\triangleq\begin{bmatrix}0_{1\times1}&-\tilde{\eta}W\tilde{B}F_0MK\tilde{C}\\ 0_{1\times1}&0_{1\times1}\end{bmatrix}\\
\tilde{\iota}_{62}&\triangleq\begin{bmatrix}0_{1\times3}\ \tilde{\eta}W\tilde{B}F_0MK\tilde{C}\ 0_{1\times1}\\ 0_{1\times3}\quad 0_{1\times1}\quad 0_{1\times1}\end{bmatrix}.
\end{aligned}
$$

Noted that the term $P\tilde{B}F_0K\tilde{C}$ in φ_1, we let $(P\tilde{B}F_0-ST)T^{-1}U\tilde{C}+SU\tilde{C}=P\tilde{B}F_0K\tilde{C}$ with $K=T^{-1}U$. Then

$$
\begin{aligned}
\varphi_1&=\alpha_1+\xi_1\xi_2+\xi_2^T\xi_1^T\\
&\le\xi_3T^{-1}\varepsilon_1\left(T^{-1}\right)^T\xi_3^T+\xi_2^T\left(\varepsilon_1^{-1}\right)^{-1}\xi_2 \qquad (24)
\end{aligned}
$$

with

$$
\begin{aligned}
\alpha_1&\triangleq\begin{bmatrix}0_{1\times1}&-SU\tilde{C}\ 0_{1\times3}\ SU\tilde{C}\ 0_{1\times4}\\ 0_{9\times1}&0_{9\times1}\ 0_{9\times3}\ 0_{9\times1}\ 0_{9\times4}\end{bmatrix}\\
\xi_1^T&\triangleq\begin{bmatrix}T^{-1^T}(P\tilde{B}F_0-ST)^T\ 0_{1\times10}\end{bmatrix}\\
\xi_2&\triangleq\begin{bmatrix}0_{1\times1}\ -U\tilde{C}\ 0_{1\times3}\ U\tilde{C}\ 0_{1\times4}\end{bmatrix}\\
\xi_3^T&\triangleq\begin{bmatrix}(P\tilde{B}F_0-ST)^T\ 0_{1\times10}\end{bmatrix}.
\end{aligned}
$$

With the similar method mentioned above, by handling the term $-\tilde{\eta}Z\tilde{B}F_0K\tilde{C}$ in φ_3 and the term $-\tilde{\eta}W\tilde{B}F_0K\tilde{C}$ in φ_5, letting $(Z\tilde{B}F_0-VT)T^{-1}U\tilde{C}+VU\tilde{C}=Z\tilde{B}F_0K\tilde{C}$ and $(W\tilde{B}F_0-GT)T^{-1}U\tilde{C}+GU\tilde{C}=Z\tilde{B}F_0K\tilde{C}$, the following inequality can be acquired:

$$
\begin{aligned}
\varphi_3&\le\alpha_2+(\tilde{\eta}\xi_2)^T\left(\varepsilon_2^{-1}\right)^{-1}(\tilde{\eta}\xi_2)\\
&\quad+\xi_4T^{-1}\varepsilon_2\left(T^{-1}\right)^T\xi_4^T \qquad (25)\\
\varphi_5&\le\alpha_3+(\tilde{\eta}\xi_2)^T\left(\varepsilon_3^{-1}\right)^{-1}(\tilde{\eta}\xi_2)\\
&\quad+\xi_5T^{-1}\varepsilon_3\left(T^{-1}\right)^T\xi_5^T \qquad (26)
\end{aligned}
$$

where

$$\alpha_2\triangleq\begin{bmatrix}0_{1\times7}&0_{1\times1}&0_{1\times2}\\ 0_{1\times7}&-\tilde{\eta}\tilde{C}^TU^T\tilde{B}^T&0_{1\times2}\\ 0_{3\times7}&0_{3\times1}&0_{3\times2}\\ 0_{1\times7}&\tilde{\eta}\tilde{C}^TU^T\tilde{B}^T&0_{1\times2}\\ 0_{4\times7}&0_{4\times1}&0_{4\times2}\end{bmatrix}$$

$$\alpha_3 \triangleq \begin{bmatrix} 0_{1\times8} & 0_{1\times1} & 0_{1\times1} \\ 0_{1\times8} & -\tilde{\eta}\tilde{C}^T U^T \tilde{B}^T & 0_{1\times1} \\ 0_{3\times8} & 0_{3\times1} & 0_{3\times1} \\ 0_{1\times8} & \tilde{\eta}\tilde{C}^T U^T \tilde{B}^T & 0_{1\times1} \\ 0_{4\times8} & 0_{4\times1} & 0_{4\times1} \end{bmatrix}$$

$$\xi_4^T \triangleq \begin{bmatrix} 0_{1\times7} & (Z\tilde{B}F_0 - GT)^T & 0_{1\times2} \end{bmatrix}$$

$$\xi_5^T \triangleq \begin{bmatrix} 0_{1\times8} & (W\tilde{B}F_0 - VT)^T & 0_{1\times1} \end{bmatrix}.$$

For calculating conveniently, the term $P\tilde{B}F_0MK\tilde{C}$ in φ_2 should be disposed. Then, enlightened by the inequality $\tilde{A}\tilde{B}^T + \tilde{B}\tilde{A}^T \le \varepsilon\tilde{A}\tilde{A}^T + \varepsilon^{-1}\tilde{B}\tilde{B}^T$, we have

$$\varphi_2 = \xi_6 M \xi_7 + \xi_7^T M^T \xi_6^T \le \xi_6 \left(\varepsilon_4^{-1}\right)^{-1} \xi_6^T + \xi_7^T \varepsilon_4^{-1} \xi_7 \quad (27)$$

where

$$\xi_6 \triangleq \begin{bmatrix} F_0^T \tilde{B}^T P & 0_{1\times9} \end{bmatrix}^T$$

$$\xi_7 \triangleq \begin{bmatrix} 0_{1\times1} & -K\tilde{C} & 0_{1\times3} & K\tilde{C} & 0_{1\times4} \end{bmatrix}.$$

Applied the same approach mentioned above, the term $Z\tilde{B}F_0MK\tilde{C}$ in φ_4 and the term $W\tilde{B}F_0MK\tilde{C}$ in φ_6 can be estimated as follows:

$$\varphi_4 \le (\tilde{\eta}\xi_7)\varepsilon_5^{-1}(\tilde{\eta}\xi_7)^T + \xi_8(\varepsilon_5^{-1})^{-1}\xi_8^T \quad (28)$$

$$\varphi_6 \le (\tilde{\eta}\xi_7)\varepsilon_6^{-1}(\tilde{\eta}\xi_7)^T + \xi_9 \left(\varepsilon_6^{-1}\right)^{-1} \xi_9^T \quad (29)$$

where

$$\xi_8 \triangleq \begin{bmatrix} 0_{1\times7} & F_0^T \tilde{B}^T Z & 0_{1\times2} \end{bmatrix}^T$$

$$\xi_9 \triangleq \begin{bmatrix} 0_{1\times8} & F_0^T \tilde{B}^T W & 0_{1\times1} \end{bmatrix}^T.$$

After that, applying Schur complement to conditions (24)–(29) and according to condition (23), conditions (12) and (13) can be guaranteed.

REFERENCES

[1] A. Sajadi, S. Zhao, K. Clark, and K. A. Loparo, "Small-signal stability analysis of large-scale power systems in response to variability of offshore wind power plants," *IEEE Syst. J.*, vol. 13, no. 3, pp. 3070–3079, Sep. 2019.

[2] H. Pan, H. Lian, C. Na, and X. Li, "Modeling and vulnerability analysis of cyber-physical power systems based on community theory," *IEEE Syst. J.*, vol. 14, no. 3, pp. 3938–3948, Sep. 2020.

[3] H. Sun, C. Peng, D. Yue, Y. L. Wang, and T. Zhang, "Resilient load frequency control of cyber-physical power systems under QoS-dependent event-triggered communication," *IEEE Trans. Syst., Man Cybern. Syst.*, vol. 51, no. 4, pp. 2113–2122, Apr. 2021.

[4] E. Tian and C. Peng, "Memory-based event-triggering H_∞ load frequency control for power systems under deception attacks," *IEEE Trans. Cybern.*, vol. 50, no. 11, pp. 4610–4618, Nov. 2020.

[5] H. Shen, S. Jiao, J. H. Park, and V. Sreeram, "An improved result on H_∞ load frequency control for power systems with time delays," *IEEE Syst. J.*, vol. 15, no. 3, pp. 3238–3248, Sep. 2021.

[6] Y. Jia, K. Meng, K. Wu, C. Sun, and Z. Y. Dong, "Optimal load frequency control for networked power systems based on distributed economic MPC," *IEEE Trans. Syst. Man Cybern. Syst.*, vol. 51, no. 4, pp. 2123–2133, Apr. 2021.

[7] H. Bevrani and T. Hiyama, "Robust decentralised PI based LFC design for time delay power systems," *Energy Convers. Manage.*, vol. 49, no. 2, pp. 193–204, 2008.

[8] W. Yao, L. Jiang, Q. Wu, J. Wen, and S. Cheng, "Delay-dependent stability analysis of the power system with a wide-area damping controller embedded," *IEEE Trans. Power Syst.*, vol. 26, no. 1, pp. 233–240, Feb. 2011.

[9] Z. Huang, J. Xia, J. Wang, Y. Wei, Z. Wang, and J. Wang, "Mixed $H_\infty/l_2 - l_\infty$ state estimation for switched genetic regulatory networks subject to packet dropouts: A persistent dwell-time switching mechanism," *Appl. Math. Comput.*, vol. 355, pp. 198–212, 2019.

[10] H. Shen, S. Jiao, J. Cao, and T. Huang, "An improved result on sampled-data synchronization of Markov jump delayed neural networks," *IEEE Trans. Syst. Man Cybern. Syst.*, vol. 51, no. 6, pp. 3608–3616, Jun. 2021.

[11] J. Zhang, S. Li, C. K. Ahn, and Z. Xiang, "Decentralized event-triggered adaptive fuzzy control for nonlinear switched large-scale systems with input delay via command-filtered backstepping," *IEEE Trans. Fuzzy Syst.*, to be published, doi: 10.1109/TFUZZ.2021.3066297.

[12] Z. Zhang *et al.*, "An event-triggered secondary control strategy with network delay in islanded microgrids," *IEEE Syst. J.*, vol. 13, no. 2, pp. 1851–1860, Jun. 2019.

[13] M. Li, S. Li, C. K. Ahn, and Z. Xiang, "Adaptive fuzzy event-triggered command-filtered control for nonlinear time-delay systems," *IEEE Trans. Fuzzy Syst.*, to be published, doi: 10.1109/TFUZZ.2021.3052095.

[14] F. Yang, J. He, and D. Wang, "New stability criteria of delayed load frequency control systems via infinite-series-based inequality," *IEEE Trans. Ind. Inform.*, vol. 14, no. 1, pp. 231–240, Jan. 2018.

[15] S. Wen, X. Yu, Z. Zeng, and J. Wang, "Event-triggering load frequency control for multiarea power systems with communication delays," *IEEE Trans. Ind. Electron.*, vol. 63, no. 2, pp. 1308–1317, Feb. 2016.

[16] J. Wang, C. Yang, J. Xia, Z. Wu, and H. Shen, "Observer-based sliding mode control for networked fuzzy singularly perturbed systems under weighted try-once-discard protocol," *IEEE Trans. Fuzzy Syst.*, to be published, doi: 10.1109/TFUZZ.2021.3070125.

[17] K. Wang, E. Tian, J. Liu, L. Wei, and D. Yue, "Resilient control of networked control systems under deception attacks: A memory-event-triggered communication scheme," *Int. J. Robust Nonlinear Control*, vol. 30, no. 4, pp. 1534–1548, 2020.

[18] Y. Wang, X. Hu, K. Shi, X. Song, and H. Shen, "Network-based passive estimation for switched complex dynamical networks under persistent dwell-time with limited signals," *J. Franklin Inst.*, vol. 357, no. 15, pp. 10921–10936, 2020.

[19] W. Qi, G. Zong, and W. X. Zheng, "Adaptive event-triggered SMC for stochastic switching systems with semi-Markov process and application to boost converter circuit model," *IEEE Trans. Circuits Syst. I., Reg. Papers*, vol. 68, no. 2, pp. 786–796, Feb. 2021.

[20] C. Peng and T. C. Yang, "Event-triggered communication and H_∞ control co-design for networked control systems," *Automatica*, vol. 49, no. 5, pp. 1326–1332, 2013.

[21] S. Li, C. K. Ahn, J. Guo, and Z. Xiang, "Neural-network approximation-based adaptive periodic event-triggered output-feedback control of switched nonlinear systems," *IEEE Trans. Cybern.*, vol. 51, no. 8, pp. 4011–4020, Aug. 2021.

[22] Y. Qi, X. Zhao, and X. Zhao, "Event-triggered control for networked switched systems subject to data asynchronization," *IEEE Syst. J.*, vol. 15, no. 4, pp. 5197–5208, Dec. 2021.

[23] M. Saeedi, J. Zarei, R. Razavi-Far, and M. Saif, "Event-triggered adaptive optimal fast terminal sliding mode control under denial-of-service attacks," *IEEE Syst. J.*, to be published, doi: 10.1109/JSYST.2021.3073816.

[24] J. Zhang and Z. Xiang, "Event-triggered adaptive neural network sensor failure compensation for switched interconnected nonlinear systems with unknown control coefficients," *IEEE Trans. Neural Netw. Learn. Syst.*, to be published, doi: 10.1109/TNNLS.2021.3069817.

[25] J. Zhang, S. Li, and Z. Xiang, "Adaptive fuzzy output feedback event-triggered control for a class of switched nonlinear systems with sensor failures," *IEEE Trans. Circuits Syst. I., Reg. Papers*, vol. 67, no. 12, pp. 5336–5346, Dec. 2020.

[26] S. Kuppusamy and Y. H. Joo, "Resilient reliable H_∞ load frequency control of power system with random gain fluctuations," *IEEE Trans. Syst. Man Cybern. Syst.*, to be published, doi: 10.1109/TSMC.2021.3049392.

[27] J. Liu, Y. Gu, L. Zha, Y. Liu, and J. Cao, "Event-triggered H_∞ load frequency control for multiarea power systems under hybrid cyber attacks," *IEEE Trans. Syst. Man Cybern. Syst.*, vol. 49, no. 8, pp. 1665–1678, Aug. 2019.

[28] Z. Wu, H. Mo, J. Xiong, and M. Xie, "Adaptive event-triggered observer-based output feedback L_∞ load frequency control for networked power systems," *IEEE Trans. Ind. Inform.*, vol. 16, no. 6, pp. 3952–3962, Jun. 2020.

[29] W. Qi, X. Yang, J. H. Park, J. Cao, and J. Cheng, "Fuzzy SMC for quantized nonlinear stochastic switching systems with semi-Markovian process and application," *IEEE Trans. Cybern.*, to be published, doi: 10.1109/TCYB.2021.3069423.

[30] W. Qi, G. Zong, and S.-F. Su, "Fault detection for semi-Markov switching systems in the presence of positivity constraints," *IEEE Trans. Cybern.*, to be published, doi: 10.1109/TCYB.2021.3096948.
[31] J. Wang, Z. Huang, Z. Wu, J. Cao, and H. Shen, "Extended dissipative control for singularly perturbed PDT switched systems and its application," *IEEE Trans. Circuits Syst. I., Reg. Papers*, vol. 67, no. 12, pp. 5281–5289, Dec. 2020.
[32] H. Shen, X. Hu, J. Wang, J. Cao, and W. Qian, "Non-fragile H_∞ synchronization for Markov jump singularly perturbed coupled neural networks subject to double-layer switching regulation," *IEEE Trans. Neural Netw. Learn. Syst.*, to be published, doi: 10.1109/TNNLS.2021.3107607.
[33] A. Argha, S. W. Su, and B. G. Celler, "Static output feedback fault tolerant control using control allocation scheme," *Int. J. Robust Nonlinear Control*, vol. 29, no. 1, pp. 98–116, 2018.
[34] Z.-Y. Feng, L. Xu, M. Wu, and J.-H. She, "H_∞ static output feedback control of 2-D discrete systems in FM second model," *Asian J. Control*, vol. 14, no. 6, pp. 1505–1513, 2011.
[35] C. Peng, J. Zhang, and H. Yan, "Adaptive event-triggering H_∞ load frequency control for network-based power systems," *IEEE Trans. Ind. Electron.*, vol. 65, no. 2, pp. 1685–1694, Feb. 2018.
[36] F. Yang, J. He, and Q. Pan, "Further improvement on delay-dependent load frequency control of power systems via truncated B-l inequality," *IEEE Trans. Power Syst.*, vol. 33, no. 5, pp. 5062–5071, Sep. 2018.
[37] L. Jiang, W. Yao, Q. Wu, J. Wen, and S. Cheng, "Delay-dependent stability for load frequency control with constant and time-varying delays," *IEEE Trans. Power Syst.*, vol. 27, no. 2, pp. 932–941, May 2012.
[38] L. Su and H. Shen, "Fault-tolerant dissipative synchronization for chaotic systems based on fuzzy mixed delayed feedback," *Neurocomputing*, vol. 151, no. 3, pp. 1407–1413, 2015.
[39] L. Zhang, T. Yang, P. Shi, and M. Liu, "Stability and stabilization of a class of discrete-time fuzzy systems with semi-Markov stochastic uncertainties," *IEEE Trans. Syst. Man Cybern. Syst.*, vol. 46, no. 12, pp. 1642–1653, Dec. 2016.
[40] T. Yang, L. Zhang, and H.-K. Lam, "H_∞ fuzzy control of semi-Markov jump nonlinear systems under σ-error mean square stability," *Int. J. Syst. Sci.*, vol. 48, no. 11, pp. 2291–2299, 2017.
[41] C. Peng, J. Li, and M. Fei, "Resilient event-triggering H_∞ load frequency control for multi-area power systems with energy-limited DoS attacks," *IEEE Trans. Power Syst.*, vol. 32, no. 5, pp. 4110–4118, Sep. 2017.
[42] D. Ding, Q.-L. Han, X. Ge, and J. Wang, "Secure state estimation and control of cyber-physical systems: A survey," *IEEE Trans. Syst. Man Cybern. Syst.*, vol. 51, no. 1, pp. 176–190, Jan. 2021.
[43] K. Liu, V. Suplin, and E. Fridman, "Stability of linear systems with general sawtooth delay," *IMA J. Math. Control Inf.*, vol. 27, no. 4, pp. 419–436, 2010.
[44] P. Park, J. W. Ko, and C. Jeong, "Reciprocally convex approach to stability of systems with time-varying delays," *Automatica*, vol. 47, no. 1, pp. 235–238, 2011.

Hao Shen (Member, IEEE) received the Ph.D. degree in control theory and control engineering from the Nanjing University of Science and Technology, Nanjing, China, in 2011.

Since 2011, he has been with the Anhui University of Technology, Ma'anshan, China, where he is currently a Professor. His research interests include stochastic hybrid systems, complex networks, fuzzy systems and control, nonlinear control.

Dr. Shen has served on the technical program committee for several international conferences. He is currently an Associate Editor/Guest Editor for several international journals, including *Journal of The Franklin Institute*, *Applied Mathematics and Computation*, *Neural Processing Letters* and *Transactions of the Institute Measurement and Control*. He was a recipient of the Highly Cited Researcher Award by Clarivate Analytics (formerly, Thomson Reuters) in 2019–2021.

Yude Xia received the M.S. degree in electrical engineering from the School of Electrical and Information Engineering, Anhui University of Technology, Ma'anshan, China, in 2021. He is currently working toward the Ph.D. degree in agricultural electrification and automation from the School of Engineering, Nanjing Agricultural University, Nanjing, China.

His research interests include switched systems, stochastic systems, and finite-time control.

Jing Wang received the Ph.D. degree in power system and automation from Hohai University, Nanjing, China, in 2019.

She is currently an Associate Professor with the Anhui University of Technology, Ma'anshan, China.

Her research interests include Markov jump nonlinear systems, singularly perturbed systems, power systems, and nonlinear control.

Ju H. Park (Senior Member, IEEE) received the Ph.D. degree in electronics and electrical engineering from the Pohang University of Science and Technology (POSTECH), Pohang, South Korea, in 1997.

From May 1997 to February 2000, he was a Research Associate with Engineering Research Center-Automation Research Center, POSTECH. He joined Yeungnam University, Kyongsan, South Korea, in March 2000, where he is currently the Chuma Chair Professor. He is a Co-author of the monographs *Recent Advances in Control and Filtering of Dynamic Systems with Constrained Signals* (Springer-Nature, 2018) and *Dynamic Systems With Time Delays: Stability and Control* (Springer-Nature, 2019) and is an Editor of an edited volume *Recent Advances in Control Problems of Dynamical Systems and Networks* (Springer-Nature, 2020). His research interests include robust control and filtering, neural/complex networks, fuzzy systems, multiagent systems, and chaotic systems. He has published a number of articles in these areas.

Prof. Park is a fellow of the Korean Academy of Science and Technology (KAST). Since 2015, he has been a recipient of the Highly Cited Researchers Award by Clarivate Analytics (formerly, Thomson Reuters) and listed in three fields, Engineering, Computer Sciences, and Mathematics, in 2019, 2020, and 2021. He also serves as an Editor of the *International Journal of Control, Automation and Systems*. He is also a Subject Editor/Advisory Editor/Associate Editor/Editorial Board Member of several international journals, including *IET Control Theory and Applications, Applied Mathematics and Computation, Journal of The Franklin Institute, Nonlinear Dynamics, Engineering Reports, Cogent Engineering*, the IEEE TRANSACTION ON FUZZY SYSTEMS, IEEE TRANSACTION ON NEURAL NETWORKS AND LEARNING SYSTEMS, and IEEE TRANSACTION ON CYBERNETICS.